ISSN 0915-633X

# NATIONAL INSTITUTE FOR FUSION SCIENCE

## On Origin and Dynamics of the Discrete NLS Equation

L. Hadžievski, M.M. Škorić and T. Sato

(Received - Nov. 10, 2000 )

NIFS-670 Nov. 2000



RESEARCH REPORT
NIFS Series

TOKI, JAPAN

# On origin and dynamics of the discrete NLS equation

Ljupčo Hadžievski [1], Miloš M. Škorić [1 2] and Tetsuya Sato [2]

[1] *Vinča Institute of Nuclear Sciences 11001 Belgrade, Serbia, Yugoslavia*

[2] *Theory and Computer Simulation Center, National Institute for Fusion Science, Toki 509-5292, Japan*

**Abstract**

We investigate soliton-like dynamics in the descrete nonlinear Schroedinger equation (DNLSE) describing the generic 3-element descrete nonlinear system with a dispersion The DNLSE (1+2) is solved on the $3 \times N$ descrete lattice, where $N$ is the variable number introduced through the descretized dispersion term. In quasi-linear and strongly nonlinear regimes the evolution shows robustness with respect to the $N$ variation. However, the intermediate regime often exhibiting chaos, appears highly sensitive to the number of descrete points, making an exact solving of the DNLSE (1+2) a dubious task. We briefly outline implications on other continuum models alike the NLSE.

KEYWORDS: discrete NLS equation, numerical simulation, solitons, chaos

## 1 Introduction

As a rule the mathematical modeling of many nonlinear systems with a different origin leads to one of the universal nonlinear evolution equations, like the nonlinear Schroedinger equation (NLS), Korteweg-de-Vries equation (KdV), Sine-Gordon equation (SG), etc. These nonlinear partial differential equations (PDEs) represent continuum models for different nonlinear systems that exhibit diverse and fascinating phenomena including *solitons, pattern formation, collapse (blow-up) solutions* and *spatio-temporal chaos.*

On the other hand, the fact that matter itself is discrete, i.e. it consists of many elementary entities, attracts the scientific interest in nonlinear discrete systems. If the spatial scale of the physical process approaches the size of the elementary entities, constituents of the physical system, a continuum approach fails and the discreteness of the system must be taken into account. In this situation the mathematical modeling of the nonlinear discrete systems leads to one of the discrete versions of the nonlinear evolution equations. In this case the origin of the discreteness comes from the very nature of the described nonlinear system and we can define the discreteness as being a *generic* one. Another way to obtain the variety of discrete nonlinear evolution equations is by applying different numerical methods (finite difference or spectral methods) in order to solve the corresponding original continuum version of various nonlinear evolution equations. Accordingly, one can find the discreteness as an *introduced* one. Thus, studies of the basic properties of the discrete nonlinear evolution equations often appear to be of a more general interest than the particular physical systems that the mathematical models describe.

The most extensively studied nonlinear evolution equation is the cubic NLS equation playing the central role in the field of plasma physics, nonlinear optics, water waves, etc. [1 11]. There are numerous discretizations of the original NLS equation leading to integrable and different non-integrable variants of the discrete NLS equations (DNLS). The obtained DNLS equations can be understood as (i) a basis for different numerical schemes for simulating the continuum NLS equation and/or (ii) a model for describing different discrete nonlinear systems of the NLS type. For example, the energy transport in molecular chains of the alpha-helix structure of proteins, the propagation of nonlinear waves in discrete electrical lattices and optical pulse propagation in nonlinear fiber arrays are all described with the discrete version of nonlinear Schroedinger equation [8–11]. In this work, we

study numerically the dynamics of the three element DNLS (1+2) equation (1 discrete plus 2 continuum variables), as an example where the both types of discreteness, generic and introduced, are present.

## 2 The cubic NLS and DNLS equations

The cubic NLS equation [1]

$$i\frac{\partial\psi}{\partial t} + \Delta\psi + 2|\psi|^2\psi = 0, \qquad (1)$$

generally arises as an asymptotic limit of a slowly varying dispersive wave envelope in a nonlinear medium. It is completely integrable via e.g. the inverse scattering transform and has an infinite number of the conserved quantities:
(i) The total energy (norm $L^2$)

$$P = \int_{-\infty}^{\infty} |\psi|^2 dV \qquad (2)$$

(ii) the Hamiltonian

$$H = \int_{-\infty}^{\infty} (|\nabla\psi|^2 - |\psi|^4) dV, \qquad (3)$$

(iii) the linear momentum

$$M = i\int_{-\infty}^{\infty} (\psi\nabla\psi^* - \psi^*\nabla\psi) dV \qquad (4)$$

... etc.

For the subcritical case (1D case: $\Delta = \frac{\partial^2}{\partial x^2}$ ) eq. (1) possesses a stable ground state soliton solution:

$$\psi_s = \frac{\lambda}{\cosh(\lambda x)} \exp(i\lambda^2 t), \qquad (5)$$

however, for the critical 2D case ($\Delta = \frac{\partial^2}{\partial x^2} + \frac{\partial^2}{\partial y^2}$) under the condition and the supercritical 3D case ($\Delta = \frac{\partial^2}{\partial x^2} + \frac{\partial^2}{\partial y^2} + \frac{\partial^2}{\partial z^2}$) for the soliton solution (5) becomes unstable and blows up (collapses) [2, 3]. From the mathematical point of view the term blow-up or collapse designates a situation where the maximum of $|\psi|$ tends to infinity (creation of a singularity) in a finite time. The singularity also indicates that the assumptions made in derivation of the equations break down, and in reality collapse, will always be prevented by the dissipation process or higher order nonlinearities. Thus, the blow-up or collapse physically represents a process of a spontaneus concentration of the wave energy in a small spatial region followed by an explosive growth of the amplitude $|\psi|$. This unique phenomenon has been observed experimentally, analytically and numerically in many nonlinear systems, but probably the best-known examples are the Langmuir wave collapse in plasma physics [4] and the self-focusing of light beams in nonlinear optics [5].

There are numerous versions of the discrete NLS equations (DNLS) which generally belong to the class of differential-difference equations (D$\Delta$E). For the 1D case there are two most popular finite difference NLS discretizations, where the origin of the discreteness could be either generic or introduced [6]:
(i) the Ablowitz-Ladik integrable DNLS (1+1) equation

$$i\frac{d\psi_n}{dt} + |\psi_n|^2(\psi_{n+1}+\psi_{n-1}) + (\psi_{n+1}+\psi_{n-1}-2\psi_n) = 0, \qquad (6)$$

(ii) non-integrable DNLS (1+1) equation

$$i\frac{d\psi_n}{dt} + 2|\psi_n|^2\psi_n + (\psi_{n+1} + \psi_{n-1} - 2\psi_n) = 0. \qquad (7)$$

A novel feature of the non-integrable DNLS equation (7) is its inherent chaotic behavior observed analytically and numerically [7, 8]. However, even the integrable version of DNLS equation (6) can show the numerically induced chaos [9, 10], because the introduced numerical errors can be considered as non-integrable perturbations of the original system. The numerically induced chaos is also found in the numerical simulations of eq. (6).

The important feature of DNLS equations (6) and (7) is the existence of stationary and localized discrete modes in an analogy with the solitons in 1D NLS equation. These discrete localized solutions known in the literature as *discrete solitons* (eq. 6) or *discrete soliton-like solutions* (eq. 7) are examples of more general phenomenon of the *discrete breathers* [11].

The more general case is DNLS (1+2) equation

$$i\frac{\partial\psi_n}{\partial t} + \frac{\partial^2\psi_n}{\partial x^2} + 2|\psi_n|^2\psi_n + (\psi_{n+1} + \psi_{n-1} - 2\psi_n) = 0,$$
$$n = 1, 2, \ldots M \qquad \psi_0 = \psi_{M+1} = 0 \qquad (8)$$

with one discrete and two continual variables. It can be derived from the NLS equation (1) in 2D where one of the variables in the operator $\Delta$ =

$\frac{\partial^2}{\partial x^2} + \frac{\partial^2}{\partial y^2}$ is discretisized e.g. variable $y$. The equation (8) arises as a mathematical model in many nonlinear discrete systems in which case the discreteness is generic. For example, it can describe the nonlinear propagation of optical pulses in linearly coupled fiber arrays [12]. In addition, to numerically solve eq. (8) by using standard finite diference or spectral methods, one also has to discretize along the continuum variable $x$. In that way, a discrete nonlinear evolution equation is obtained, where the both types of discreteness, generic and introduced, have appeared.

The equation (8) is non-integrable, if $M > 2$ ($M$ is the number of elements of DNLS equation) and it is known to possess three conserved quantities
(i) total energy

$$P = \sum_n \int_{-\infty}^{\infty} |\psi_n|^2 dx, \tag{9}$$

(ii) Hamiltonian

$$H = \sum_n \int_{-\infty}^{\infty} (|\psi_n - \psi_{n-1}|^2 + |\psi_{n,x}|^2 - |\psi_n|^4) dx, \tag{10}$$

(iii) momentum in $x$

$$M_x = \sum_n \int_{-\infty}^{\infty} (\psi \psi^*_{n,x} - \psi^*_n \psi_{n,x}) dx. \tag{11}$$

Compared with the continuum 2D NLS equation, equation (8) exhibits a novel unique feature: existence of multidimensional soliton-like solutions localized in both dimensions, discrete and continual [13].

Another difference from the standard continuum NLS equation is that the DNLS equation (8) shows no singular behaviour. Instead, the quasi-collapse takes place, which is closely related to the collapse phenomenon in two-dimensional NLS; however for DNLS, the solution, instead toward a singularity, evolves to stable multidimensional soliton-like solutions [14]. Accordingly, a practical new method for optical pulse amplification and compresson, based on the quasi-collapse of the optical pulses, in a linearly coupled nonlinear optical fiber array, was proposed in ref. [14].

For the three element DNLS equation ($M = 3$) one exact analytical, anti-symmetric soliton-like solution is found [15]

$$\psi_1 = -\psi_3 = \frac{\lambda}{\cosh(\lambda x)} \exp(i\lambda^2 t), \quad \psi_2 = 0, \tag{12}$$

as well as, two approximate symmetric soliton-like solutions, with:
(i) energy concentrated along the central element with linear waves in the side elements

$$\psi_2 = \frac{\sqrt{2+\lambda^2}}{\cosh(x\sqrt{2+\lambda^2})} \exp(i\lambda^2 t). \tag{13}$$

$$\psi_1 = \psi_3 = \frac{1}{2\sqrt{2+\lambda^2}} [e^{x\sqrt{2+\lambda^2}} \ln(1 + e^{-2x\sqrt{2+\lambda^2}}) + e^{-x\sqrt{2+\lambda^2}} \ln(1 + e^{2x\sqrt{2+\lambda^2}})] \exp(i\lambda^2 t), \tag{14}$$

(ii) energy concentrated along the side elements and a linear wave in the central one

$$\psi_1 = \psi_2 = \frac{\sqrt{2+\lambda^2}}{\cosh(x\sqrt{2+\lambda^2})} \exp(i\lambda^2 t). \tag{15}$$

$$\psi_2 = \frac{1}{\sqrt{2+\lambda^2}} [e^{x\sqrt{2+\lambda^2}} \ln(1 + e^{-2x\sqrt{2+\lambda^2}}) + e^{-x\sqrt{2+\lambda^2}} \ln(1 + e^{2x\sqrt{2+\lambda^2}})] \exp(i\lambda^2 t), \tag{16}$$

Based on the existence of the above symmetric soliton-like solutions, a bistable optical switching system in a form of three collinear, linearly coupled nonlinear fibers (array) was proposed [14].

## 3 A numerical method

There are numerous well-developed finite difference and spectral numerical methods [16, 17] with different features in terms of accuracy, stability, time-consumption, memory requirements, etc., for simulating the NLS equation. However, it appears that not all of these methods are suitable for the generalization to obtain the high performance numerical method for solving the DNLS equation (8). For that purpose, the well-known split-step Fourier method, originally developed for the numerical solution of the standard NLS equation, has been the best candidate, which fits our requirements for an efficient spectral numerical method for the DNLS simulation. We can rewrite the DNLS equation (8) in a compact form as

$$i\frac{\partial \mathbf{U}}{\partial z} = \hat{L}\mathbf{U} + \hat{N}\mathbf{U}, \tag{17}$$

where $\mathbf{U}$ is the single column matrix (vector) and contains the complex mode amplitudes

$$\mathbf{U} = |\psi_1 \psi_2 \dots \psi_M|^{\mathbf{T}}, \tag{18}$$

$\hat{L}$ is the linear differential operator with a three-diagonal structure

$$\hat{L} = \begin{vmatrix} 2-\frac{\partial^2}{\partial x^2} & -1 & 0 & \dots & 0 \\ -1 & 2-\frac{\partial^2}{\partial x^2} & -1 & & \vdots \\ 0 & -1 & 2-\frac{\partial^2}{\partial x^2} & -1 & 0 \\ \vdots & & & & -1 \\ 0 & \dots & 0 & -1 & 2-\frac{\partial^2}{\partial x^2} \end{vmatrix}_{M\times M}, \tag{19}$$

and $\hat{N}$ is the diagonal nonlinear operator

$$\hat{N} = -2 \begin{vmatrix} |\psi_1|^2 & 0 & \dots & 0 \\ 0 & |\psi_2|^2 & & \vdots \\ \vdots & & & 0 \\ 0 & \dots & 0 & |\psi_M|^2 \end{vmatrix}_{M\times M}. \tag{20}$$

The basic idea of the split-step Fourier method is the assumption that over a small time step ($\Delta t = h$) the linear ($\hat{L}$) and nonlinear ($\hat{N}$) operators act independently. More specifically, evolution from $t$ to $t+h$ is carried out in two steps (Fig. 1.). In the first step the nonlinear operator ($\hat{N}$) acts alone ($\hat{L}=0$) and the equation (17) is reduced to

$$i\frac{\partial \mathbf{U}}{\partial z} = \hat{N}\mathbf{U}. \tag{21}$$

In the second step the linear operator ($\hat{L}$) acts alone ($\hat{N}=0$) and equation (17) is reduced to

$$i\frac{\partial \mathbf{U}}{\partial z} = \hat{L}\mathbf{U}. \tag{22}$$

The formal solution of the equation (21) is given with

$$\mathbf{U}(t+h,x) = \mathbf{U}(t,x)\exp[-i\int_t^{t+h}\hat{N}(t,x)dt]. \tag{23}$$

The equation (23) is implicit since $\hat{N}$ depends on $\mathbf{U}$ and its implementation in the numerical procedure is not so simple, because it is necessary to follow an iterative procedure. However, the iteration is time consuming and only one or two iterations are used in practice.

In order to solve eq. (22) we can apply the Fast Fourier Transform (FFT) technique with respect to variable $x$ to derive a system of ordinary differential equations with constant coefficients

$$i\frac{d\mathbf{U}(\omega,t)}{dt} = \hat{L}(\omega)\mathbf{U}(\omega.t), \tag{24}$$

(24) with the formal solution in a matrix form

$$\mathbf{U}(\omega.t+h) = \exp[-i\hat{L}(\omega)h]\mathbf{U}(\omega,t). \tag{25}$$

The matrix has $M$ different eigenvalues and consequently its Jordan matrix is diagonal. This fact gives us opportunity to calculate the matrix exponential function $\exp[-i\hat{L}(\omega)h]$ in the form of matrix $\mathbf{M}(\omega,h)$, which reduces the calculations of $\mathbf{U}(\omega,t+h)$ with equation (25) to a simple matrix multiplication

$$\mathbf{U}(\omega,t+h) = \mathbf{M}(\omega.h)\mathbf{U}(\omega,t). \tag{26}$$

The calculation of matrix $\mathbf{M}(\omega,h)$ is time consuming due to the large number of elementary operations proportional to $M^2$. However, the fact that matrix does not depend on $t$ allows one to calculate it only once at the beginning of the numerical simulation. Further in time, the same matrix is used in each integration step. With this procedure we have significantly reduced the simulation time and allowed, within the acceptable computing time (10-12 hours), to perform short scale simulations with several hundred elements, or large scale simulations with several elements, using the personal computer PII.

The error of the method is of the second order in the step size ($\sim h^2$), and can be checked upon by using the conserved quantities and defined by (9) and (10). The accuracy of our split-step Fourier method can be improved up to the third order, by using the following integration scheme over the one time step $h$ (Fig. 2.):

1) integration over the interval $[t, t+\frac{h}{2}]$ with the linear operator (26),

2) integration over the interval $[t, t+h]$ with the nonlinear operator (23),

3) integration over the interval $[t+\frac{t}{2}, t+h]$ again with the linear operator (26).

However, the improved accuracy is paid back through an extra FFT and one matrix multiplication per each integration step. On the other hand, this scheme allows one to use larger integration step with the same accuracy, while as a final result the

total simulation time appears to be approximately equal in both numerical schemes.

## 4 Numerical results

In order to study different dynamical regimes of the soliton dynamics, launched into the central element of the three-element DNLS, we have performed a numerical simulation of the equation (8) using our generalized split-step Fourier method.

We have assumed the periodic boundary conditions with respect to $x$, which implies the application of the FFT procedure, with continuos monitoring of the conserved quantities: the total energy $P$ (9) and the Hamiltonian $H$ (10).

As an initial condition ($t = 0$), we launch the NLS soliton into the central element

$$\psi_2 = \frac{\lambda_0}{\cosh(\lambda_0 x)}, \qquad \psi_1 = \psi_3 = 0. \qquad (27)$$

for different values of the initial amplitude $\psi_2(0) = \lambda_0 = 0.5; 1.25; 1.80; 2.00; 2.05; 2.25; 3.00; 4.00$ sampled on the period $L_x$ with $N$ points. The product $L_x\lambda_0$ is kept constant, in order to spatially accomodate the solitons with different amplitudes, in the same way, at the periodicity length $L_x$.

In the small amplitude region, i.e. $\lambda = 0$ a linear response of the system is observed, in agreement with the linear analytical solution of (8). The dominant process is the energy exchange between the central element and its two neighbours (Fig. 3.), followed by a weak longitudional dispersion (Fig. 4). It is actually a quasiperiodic regime, as seen in the 2-torus phase attractor (Fig. 5) with two incommensurate frequencies in the clean discrete spectrum given in Fig. 6. These results are very similar to earlier ones, numerically found in [1] for the DNLS (1+1) equation without a dispersion term (7); also, experimentally observed in [18].

Increase of the initial amplitude brings a continuous transition, as seen in the phase diagrams and amplitude spectra, while in the intermediate region $2.00 < \lambda_0 < 2.05$, one can find mode-locking, aperiodic and possibly chaotic regimes. In this case a characteristic toroidal attractor (Fig. 5) and the discretness of the spectra (Fig. 6) are lost and small variation of the initial amplitude brings a significant difference in the system dynamics (Fig 7) The existance of this regime was predicted numerically in [7] and [8] for the DNLS (1+1) equation without the dispersion (7): i.e. with the generic 1D -discreteness of the system. These results are in a plausible agreement with ours, although the dynamics of the system [7, 8] is defined through a competition of nonlinearity and discreteness, while in our case, interaction is inherently more complex, with the nonlinearity, descreteness and dispersion competing between each other. More precisely, by solving our DNLS (1+2) system we have to encounter an additional descrete dimension in comparison with the earlier DNLS (1+1) model.

Further amplitude increase brings back the dynamics to a quasiperiodic and eventually to a single-periodic, limit-cycle regime (Fig. 5) with a single spectral line (Fig. 6). In this case, it is possible to recognize the analytical soliton-like solution given by (13) and (14). The calculated values for the soliton eigen-frequency $\lambda^2$ and amplitude $\sqrt{2+\lambda^2}$, from the simulation match the corresponding analytical values given by (13) and (14).

We also note that, starting from the initial condition (27), it is not possible to reach the anti-symmetric solution (12) and the other symmetric soliton-like solution (15) and (16).

All three, qualitatively different dynamical regimes found in our simulation of the DNLS (1+2) equation also exist in the dynamics of DNLS (1+1) equation. However, the presence of the dispersion in the DNLS equation (1+2) which is handled with the FFT routine in our numerical simulation means that in our system an additional introduced discrete dimension is present. Thus, one can expect to find a dynamical regime where numerically induced chaos, as described in [9, 10] is present. The straightforward way is to check the sensitivity of the simulation results with respect to the number of the sampling ponts (number of harmonics in FFT).

Our numerical studies show that in the linear regime $\lambda \ll 2.00$ and in a strongly nonlinear regime $\lambda_0 \gg 2.00$, there is no sensitivity on $n$ and no basic difference between results obtained for a different number of sampling points is found. However, the situation is rather different in the intermediate, chaotic like regime. We have performed several numerical runs with a different number of sampling points $N = 128; 256; 512; 768; 1024; 2048$ for the same initial condition in a form of the NLS soliton (27) with $\lambda = 2.00$ keeping all other parameters fixed at the values given in the earlier simu-

lation (Fig. 5 and 6.) with $N = 1024$. The simulation results are shown in Fig. 8 in a form of phase diagrams and corresponding power spectra of the maximal amplitude in the central element (first and second columns) and in the neighbor element (third and fourth columns). Further, in Fig. 9, the space-time evolution of the amplitude in the central element for three different numbers of sampling points ($N = 768; 1024; 2048$) is shown. It is obvious that a qualitative difference exists, between results with different $N$. It is also plausible to expect that the introduced discreteness is responsible for those differences. Accordingly, the simulations results can only be regarded as correct, if we assume that the complete discreteness in the system is generic, which means that above DNLS equation describes a particular discrete system with a given number of elements in the 2D lattice (in our case $3 \times 128, 3 \times 256, \ldots$).

## 5 Conclusion

We have numerically studied in detail, the evolution of the soliton-like pulses in the framework of the descrete nonlinear Schroedinger equation describing the generic three-element descrete nonlinear system (trimer) with a dispersion. The DNLS (1+2) equation was solved in the standard way on the $3 \times N$ descrete lattice, where $N$ is variable number of points introduced through the descretization of the dispersion term. We have simulated the system dynamics with the soliton-like pulse initially launched into the central element. In quasi-linear and strongly nonlinear regimes the robustness with respect to the $N$ number is found. However, the intermediate regime exhibiting quasi-periodic and often chaotic dynamics, appears highly sensitive to the number of descrete points, making an exact solving of the DNLS (1+2) equation a dubious task. In this case, the correct solution can be expected only if we consider a generic 2-dimensional descrete system with a given fixed number of elements. However, if our task is to descretize a continuum variable with a number of points, our numerical approach can fail and becomes questionable in the intermediate regime, as seen in the above DNLS (1+2) simulation. In addition, these conclusions can be possibly extended to other finite-difference and spectral numerical schemes with the similar background of the introduced discreteness.

It is to be expected that this situation is not only typical for the DNLS equation but also for other types of discrete nonlinear evolution equations. More generally, this problem is of an additional relevance, because it can possibly emerge in different numerical schemes aims to simulate various continuum nonlinear PDE's in two and three dimensions.


### Acknowledgments

We thank Nikola Alić for his contribution in developing the numerical scheme and the computer code used in this paper. One of us (M.M.Š) acknowledges with gratitude the visiting professorship granted by the Ministry of Education, Science and Culture of Japan. This work was supported in parts by the Ministry of Science and Technology of Serbia, Project 01E11.


# References


[1] V. E. Zakharov and A. B. Shabat, Sov. Phys. JETP **34**, 62 (1972).

[2] Lj. R. Hadžievski, M. M.Škorić, A. M. Rubenchik, E. G. Shapiro and S. K. Turitsin, Phys. Rev A **42**, 3651 (1990).

[3] J. J. Rasmussen and K. Rypdal, Phys. Scr. **33**, 481 (1986).

[4] V. E. Zakharov, Sov. Phys. JETP **35**, 908 (1972).

[5] S. A. Khmanov, A. P. Sukhorukov and R. V. Khokhlov, Sov. Phys. Usp. **10**, 609 (1968).

[6] M. J. Ablowitz and J. F. Ladik, J. Math. Phys. **17**, 1011 (1976).

[7] J. C. Eilbeck, P. S. Lomdahl and A. C. Scott, Physica D **16**, 318 (1985).

[8] N. Finlayson, K. Blow, L. Bernstein and K. DeLong, Phys. Rev. A **48**, 3863 (1993).

[9] B. M. Herbst and M. J. Ablowitz, Phys. Rev. Lett. **62**, 2065 (1989).

[10] M. J. Ablowitz, C. Schober and B. M. Herbst Phys. Rev. Lett. **71**, 2683 (1993).

[11] S. Flach and C. R. Willis, Phys. Rep. **295**, 182 (1998).. D. Henning and G. P. Tsironis, Phys. Rept. **307**, 334 (1999)

[12] A. B. Aceves, G. G. Luther, C. De Angelis, A. M. Rubenchik and S. K. Turitsyn, Phys. Rev Lett. **75**, 73 (1995).

[13] A. B. Aceves, C. De Angelis, A. M. Rubenchik and S. K. Turitsyn, Opt. Lett. **19**, 329 (1994).

[14] A. B. Aceves, G. G. Luther, C. De Angelis, A. M. Rubenchik and S. K. Turitsyn, Opt.Fib. Tech. **1**, 244 (1995).

[15] A. B. Aceves and M. Santagiustina, Phys Rev. E **56**, 1113 (1997).

[16] T. R. Taha and M. J. Ablowitz, J. Comput. Phys. **55**, 203 (1984).

[17] B. Fornberg and T. A. Driscoll, J. Comput. Phys. **155**, 456 (1999).

[18] H. S. Eisenberg, Y. Silberberg, R. Morandotti, A. R. Boyd and J. S. Aitchison, Phys. Rev. Lett. **81**, 3383 (1998)

Figure captions

**Fig. 1.** One step integration scheme.

**Fig. 2.** Two steps integration scheme.

**Fig. 3.** Time evolution of the maximal amplitudes in the central element (solid line) and in the neighbor elements (dashed line) for the soliton launched into the central element with the initial amplitude $\lambda_0 = 0.5$.

**Fig. 4.** Fragment of the space time evolution of the soliton launched into the central element with the initial amplitude $\lambda_0 = 0.5$.

**Fig. 5.** Phase diagrams of the maximum of the amplitude in the central element of the soliton launched into the central element with different initial amplitudes.

**Fig. 6.** Power-spectra corresponding to the phase diagrams shown on Fig. 5.

**Fig. 7.** The space–time evolution of the solitons launched into the central element with two close initial amplitudes a) $\lambda_0 = 2.00$ b) $\lambda_0 = 2.05$.

**Fig. 8.** Phase diagrams and corresponding power spectra of the maximal amplitude in the central element (first and second columns) and in the neighbor elements (third and fourth colomns) for a different number of sampling points $N$ of the soliton launched into the central element with the initial amplitude $\lambda = 2.00$.

**Fig. 9.** The space–time evolution of the solitons launched into the central element with the initial amplitude $\lambda_0 = 2.00$ with three different number of sampling points: a) $N = 768$, b) $N = 1024$ and c) $N = 2046$.

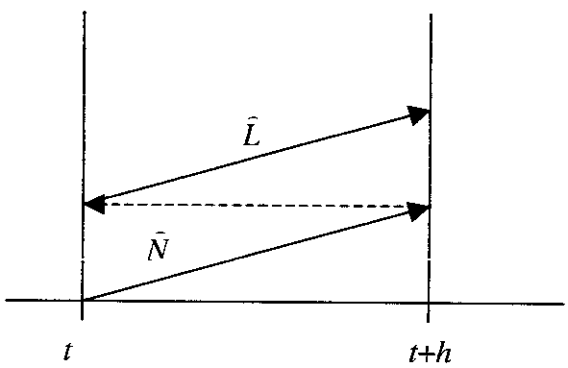


Fig. 1

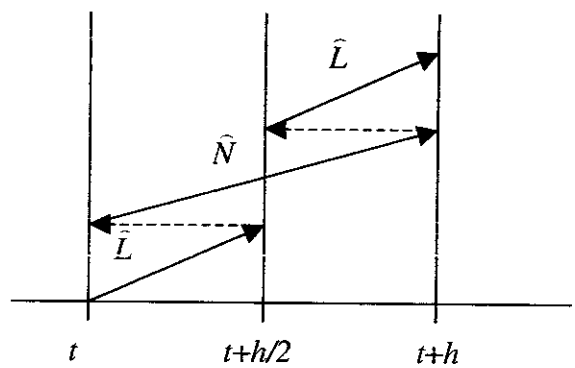


Fig. 2.

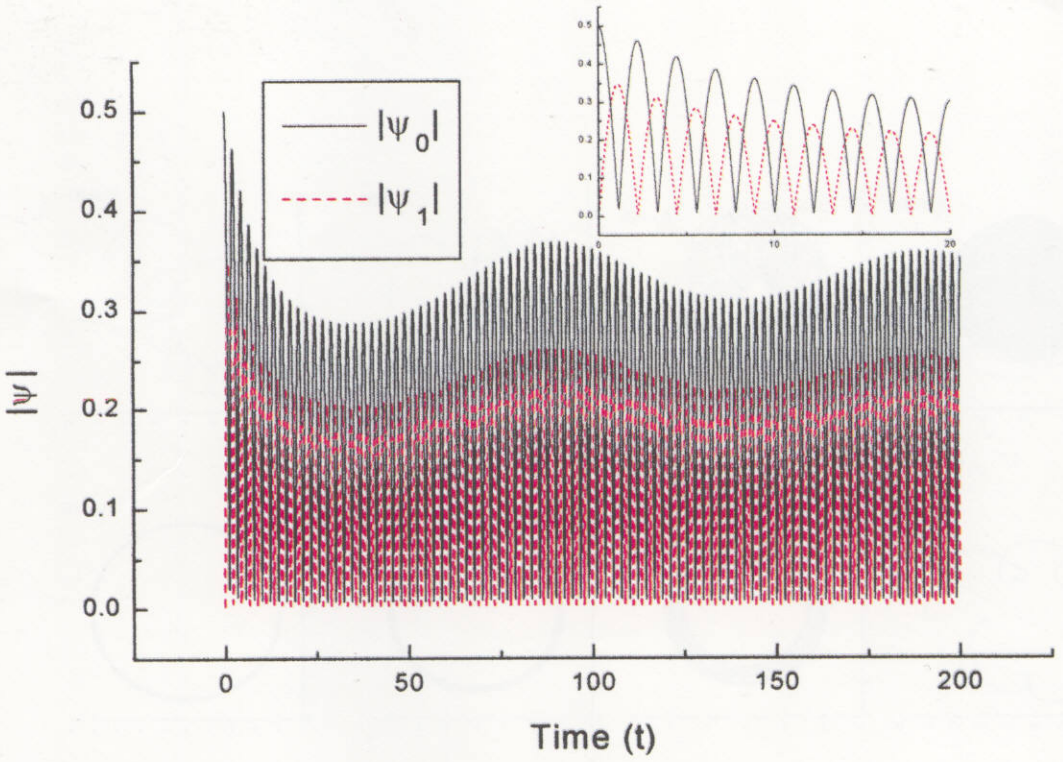


Fig. 3. Time evolution of the maximal amplitudes in the central element (solid line) and in the neighbor element (dashed line).

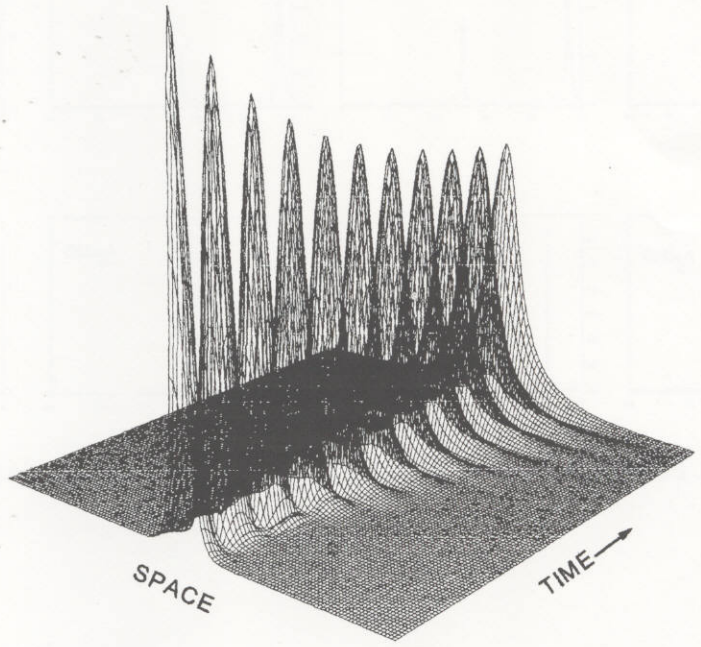


Fig. 4. The space-time evolution of the soliton launched into the central element with the initial amplitude $\lambda_0 = 0.5$.

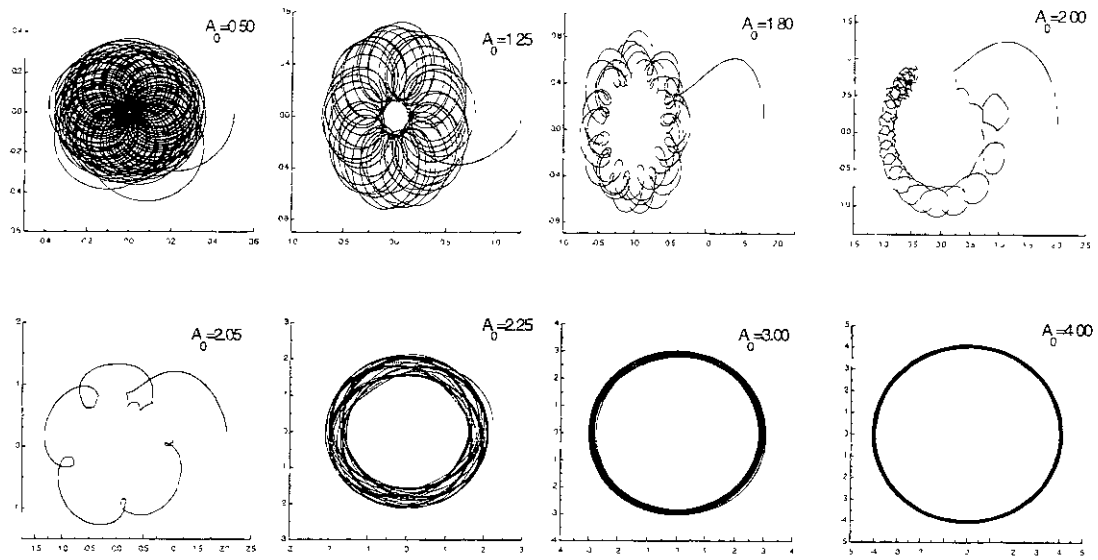


Fig. 5. Phase diagrams of the maximal amplitude in the central element.

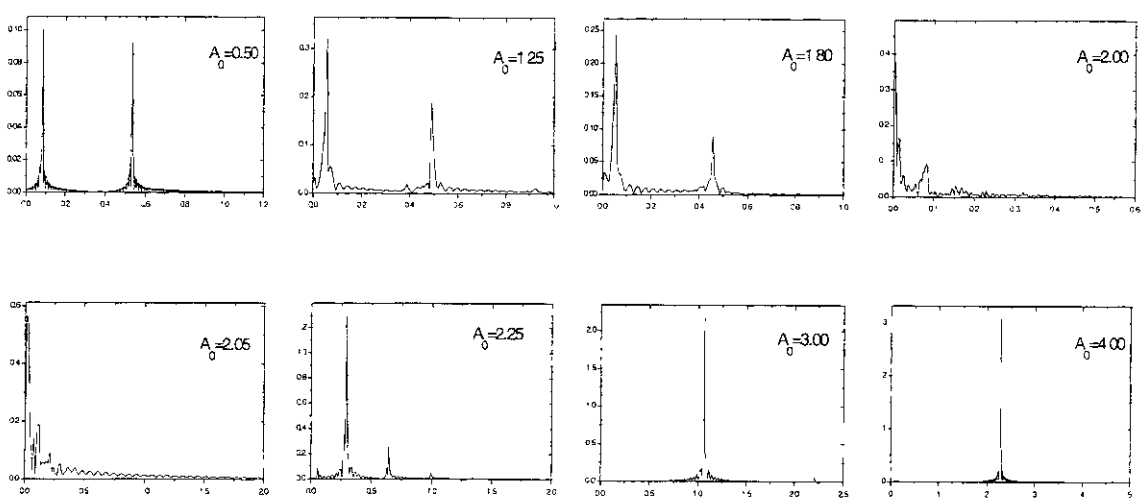


Fig. 6. Power-spectra corresponding to phase diagrams shown in Fig. 5.

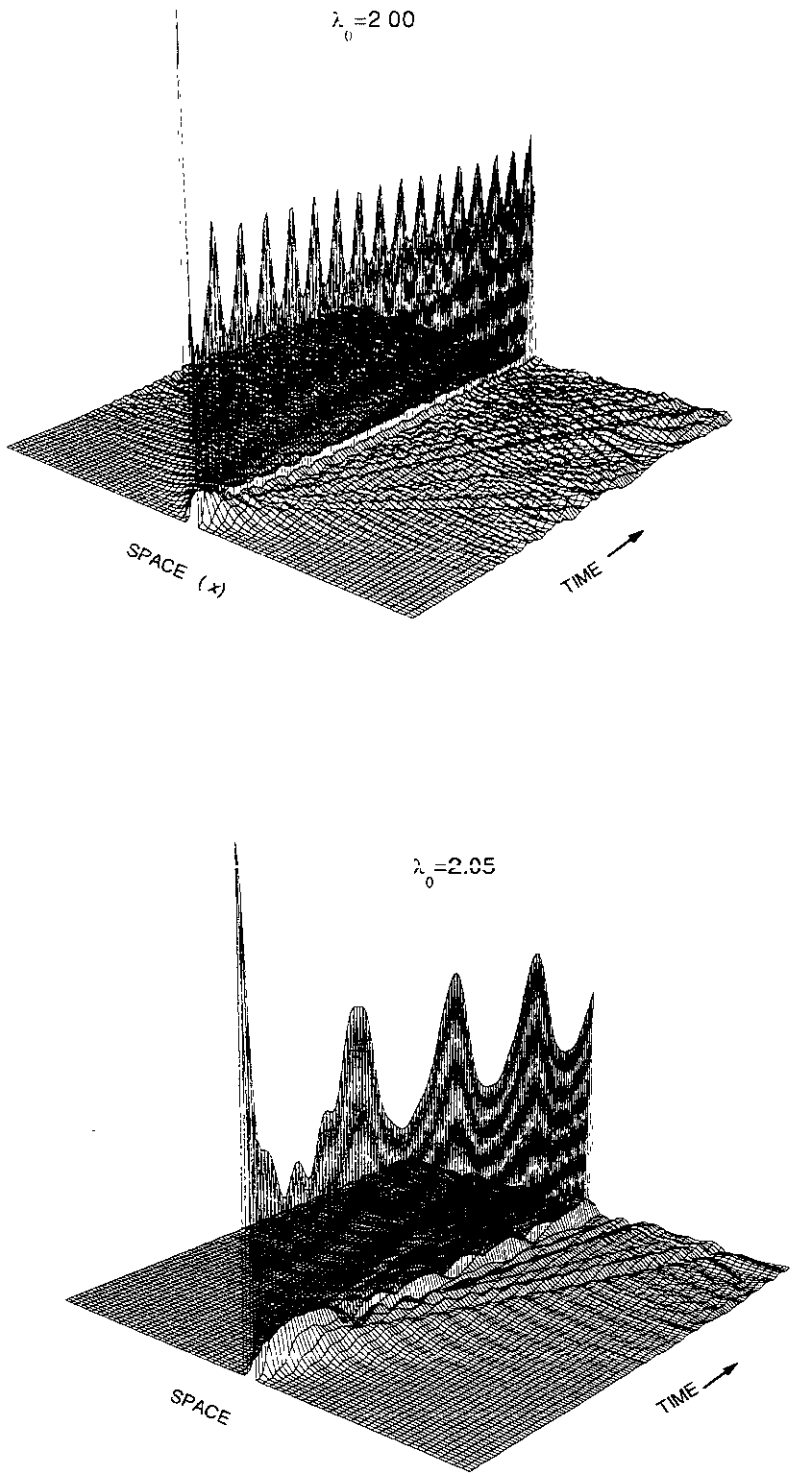


Fig. 7. Space-time evolution near the intermediate regime for two close values of the initial amplitude: $\lambda_0 = 2.00$ and $\lambda_0 = 2.05$.

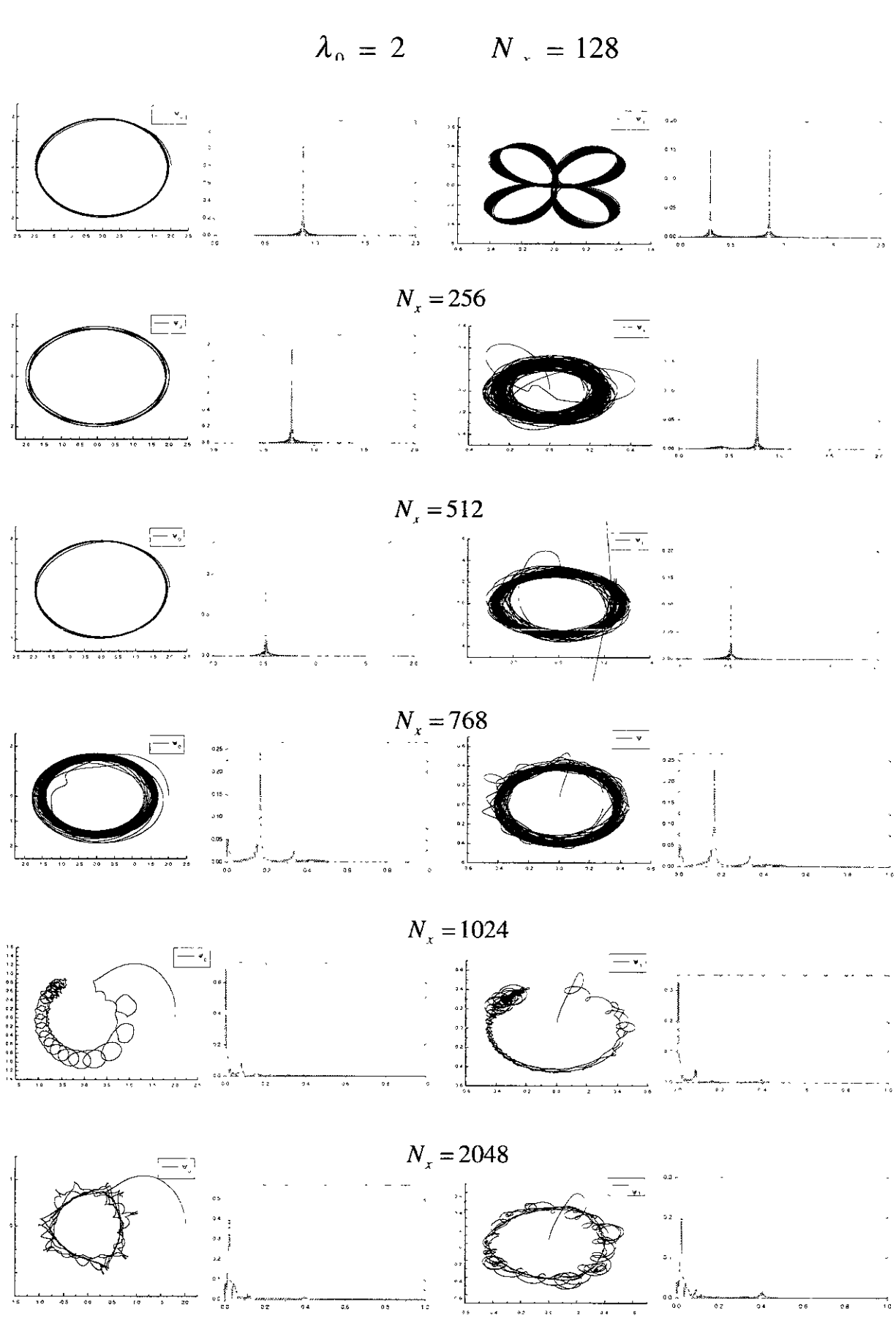


Fig. 8. Phase diagrams and corresponding power spectra of the maximal amplitude in the central element (first and second columns) and in the neighbor element (third and fourth columns).

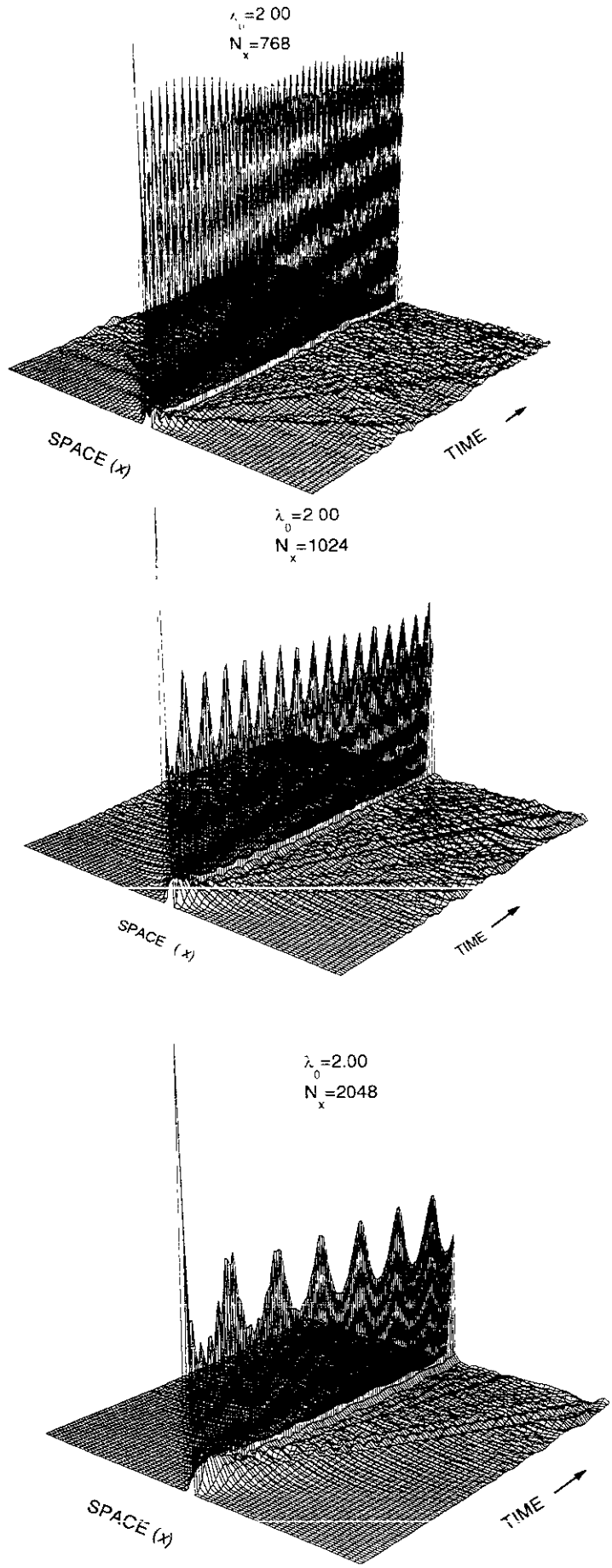


Fig. 9. Space-time evolution near the intermediate regime $\lambda_0 = 2.00$ for $N = 768,1024,2048$ points.

## Recent Issues of NIFS Series

NIFS-657 M Sasao, S Murakami, M Isobe, A V Krasilnikov, S Iidetka, K Itoh, N Nakajima, M Osakabe, K Saito, I Seki, Y Takeiri, T Watari, N Ashikawa, P deVaries, M Emoto, H Funaba, M Goto, K Ida, H Idei, K Ikeda, S Inagaki, N Inoue, S Kado, O Kaneko, K Kawahata, K Khlopenkov, T Kobuchi, A Komori, S Kubo, R Kumazawa, S Masuzaki, T Minami, J Miyazawa, T Morisaki, S Morita, S Muto, T Mutoh, Y Nagayama, Y Nakamura, H Nakanishi, K Narihara, K Nishimura, N Noda, T Notake, Y Liang, S Ohdachi, N Ohyabu, Y Oka, T Ozaki, R O Pavlichenko, B J Peterson, A Sagara, S Sakakibara, R Sakamoto, H Sasao4, K Sato, M Sato, T Shimozuma, M Shoji, H Suzuki, M Takechi, N Tamura, K Tanaka, K Toi, T Tokuzawa, Y Torii, K Tsumori, H Yamada, I Yamada, S Yamaguchi, S Yamamoto, M Yokoyama, Y Yoshimura, K Y Watanabe and O Motojima
Study of Energetic Ion Transport in the Large Helical Device Sep 2000
(IAEA-CN-77/EX9/1)

NIFS-658 B J Peterson, Y Nakamura, K Yamazaki, N Noda, J Rice, Y Takeiri, M Goto, K Narihara, K Tanaka, K Sato, S Masuzaki, S Sakakibara, K Ida, H Funaba, M Shoji, M Osakabe, M Sato, Yuhong Xu, T Kobuchi, N Ashikawa, P deVries, M Emoto, H Idei, K Ikeda, S Inagaki, N Inoue, M Isobe, S Kado, K Khlopenkov, S Kubo, R Kumazawa, T Minami, J Miyazawa, T Morisaki, S Murakami, S Muto, T Mutoh, Y Nagayama, H Nakanishi, K Nishimura, T Notake, Y Liang, S Ohdachi, Y Oka, T Ozaki, R O Pavlichenko, A Sagara, K Saito, R Sakamoto, H Sasao, M Sasao, I Seki, T Shimozuma, H Suzuki, M Takechi, N Tamura, K Toi, T Tokuzawa, Y Torii, K Tsumori, I Yamada, S Yamaguchi, S Yamamoto, M Yokoyama, Y Yoshimura, K Y Watanabe, T Watari, K Kawahata, O Kaneko, N Ohyabu, H Yamada, A Komori, S Sudo, O Motojima
Impurity transport induced oscillations in LHD Sep 2000
(IAEA-CN-77/EXP5/27)

NIFS-659 T Satow, S Imagawa, N Yanagi, K Takahata, T Mito, S Yamada, H Chikaraishi, A Nishimura, I Ohtake, Y Nakamura, S Satoh, O Motojima
Achieved Capability of the Superconducting Magnet system for the Large Helical Device Sep 2000
(IAEA-CN-77/FTP1/15)

NIFS-660 T Watari, T Mutoh, R Kumazawa, T Seki, K Saito, Y Torii, Y P Zhao, D Hartmann, H Idei, S Kubo, K Ohkubo, M Sato, T Shimozuma, Y Yoshimura, K Ikeda, O Kaneko, Y Oka, M Osakabe, Y Takeiri, K Tsumori, N Ashikawa, P C deVries, M Emoto, A Fukuyama, H Funaba, M Goto, K Ida, S Inagaki, N Inoue, M Isobe, K Itoh, S Kado, K Kawahata, T Kobuchi, K Khlopenkov, A Komori, A Krasilnikov, Y Liang, S Masuzaki, K Matsuoka, T Minami, J Miyazawa, T Morisaki, S Morita, S Murakami, S Muto, Y Nagayama, Y Nakamura, H Nakanishi, K Narihara, K Nishimura, N Noda, A T Notake, S Ohdachi, N Ohyabu, H Okada, M Okamoto, T Ozaki, R O Pavlichenko, B J Peterson, A Sagara, S Sakakibara, R Sakamoto, H Sasao, M Sasao, K Sato, S Satoh, T Satow, M Shoji, S Sudo, H Suzuki, M Takechi, N Tamura, S Tanahashi, K Tanaka, K Toi, T Tokuzawa, K Y Watanabe, T Watanabe, H Yamada, I Yamada, S Yamaguchi, S Yamamoto, K Yamazaki, M Yokoyama, Y Hamada, O Motojima, M Fujiwara,
The Performance of ICRF Heated Plasmas in LHD Sep 2000
(IAEA-CN-77/EX8/4)

NIFS-661 K Yamazaki, K Y Watanabe, A Sagara, H Yamada, S Sakakibara, K Narihara, K Tanaka, M Osakabe, K Nishimura, O Motojima, M Fujiwara, the LHD Group
Helical Reactor Design Studies Based on New Confinement Scalings Sep 2000
(IAEA-CN-77/ FTP 2/12)

NIFS-662 T Hayashi, N Mizuguchi, H Miura and T Sato
Dynamics of Relaxation Phenomena in Spherical Tokamak Sep 2000
(IAEA-CN-77THP2/13)

NIFS-663 H Nakamura and T Sato, H Kambe and K Sawada and T Saiki
Design and Optimization of Tapered Structure of Near-field Fiber Probe Based on FDTD Simulation Oct 2000

NIFS-664 N Nakajima,
Three Dimensional Ideal MHD Stability Analysis in $L$=2 Heliotron Systems Oct 2000

NIFS-665 S Fujiwara and T Sato
Structure Formation of a Single Polymer Chain I Growth of trans Domains Nov 2000

NIFS-666 S Kida,
Vortical Structure of Turbulence Nov 2000

NIFS-667 H Nakamura, S Fujiwara and T Sato
Rigidity of Orientationally Ordered Domains of Short Chain Molecules Nov 2000

NIFS-668 T Mutoh, R Kumazawa, T Seki, K Saito, Y Torii, F Shimpo, G Nomura, T Watari, D A Hartmann, M Yokota, K Akaishi, N Ashikawa, P deVries, M Emoto, H Funaba, M Goto, K Ida, H Idei, K Ikeda, S Inagaki, N. Inoue, M Isobe, O Kaneko, K Kawahata, A Komori, T Kobuchi, S Kubo, S Masuzaki, T Morisaki, S Morita, J Miyazawa, S Murakami, T Minami, S Muto, Y Nagayama, Y Nakamura, H Nakanishi, K Narihara, N Noda, K Nishimura, K Ohkubo, N Ohyabu, S Ohdachi, Y Oka, M Osakabe, T Ozaki, B J Peterson, A Sagara, N Sato, S Sakakibara, R Sakamoto, H Sasao, M Sasao, M Sato, T Shimozuma, M Shoji, S Sudo, H Suzuki, Y Takeiri, K Tanaka, K Toi, T Tokuzawa, K Tsumori, K Y Watanabe, I Watanabe, H Yamada, I Yamada, S Yamaguchi, K Yamazaki, M Yokoyama, Y Yoshimura, Y Hamada, O Motojima, M Fujiwara
Fast- and Slow-Wave Heating of Ion Cyclotron Range of Frequencies in the Large Helical Device Nov 2000

NIFS-669 K Mima, M S Jovanovic, Y Sentoku, Z-M Sheng, M M Skoric and T Sato,
Stimulated Photon Cascade and Condensate in Relativistic Laser-plasma Interaction, Nov 2000

NIFS-670 L Hadzievski, M M Skoric and T Sato,
On Origin and Dynamics of the Discrete NLS Equation Nov 2000